Physics opportunities at RHIC and LHC

S. Scherer, S. A. Bass*, M. Belkacem, M. Bleicher, J. Brachmann, A. Dumitru†, C. Ernst, L. Gerland, N. Hammon, M. Hofmann, J. Konopka, L. Neise, M. Reiter, S. Schramm, S. Soff, C. Spieles‡, H. Weber, D. Zschiesche, J.A. Maruhn, H. Stöcker, W. Greiner

Institut für Theoretische Physik, Johann Wolfgang Goethe-Universität
Robert Mayer-Str. 8–10
D-60054 Frankfurt am Main, Germany
* *present address: Department of Physics, Duke University, Durham, USA*
† *present address: Physics Department, Yale University, New Haven, USA*
‡ *present address: Lawrence Berkeley Laboratory, Berkeley, USA*

Abstract. Nonequilibrium models (three-fluid hydrodynamics, UrQMD, and quark molecular dynamics) are used to discuss the uniqueness of often proposed experimental signatures for quark matter formation in relativistic heavy ion collisions from the SPS via RHIC to LHC. It is demonstrated that these models – although they do treat the most interesting early phase of the collisions quite differently (thermalizing QGP vs. coherent color fields with virtual particles) – all yield a reasonable agreement with a large variety of the available heavy ion data. Hadron/hyperon yields, including J/Ψ meson production/suppression, strange matter formation, dileptons, and directed flow (bounce-off and squeeze-out) are investigated. Observations of interesting phenomena in dense matter are reported. However, we emphasize the need for systematic future measurements to search for simultaneous irregularities in the excitation functions of several observables in order to come close to pinning the properties of hot, dense QCD matter from data. The role of future experiments with the STAR and ALICE detectors is pointed out.

INTRODUCTION

The study of relativistic heavy ion collisions [1] offers a unique chance to explore the properties of hot and dense elementary matter. Throughout his scientific life, Klaus Kinder-Geiger has given new, creative and stimulating impulses to this exciting field of physics [2]. In the last years of his life, he had focused his attention on the very early phase of such collisions, when most of the energy is transfered to partonic degrees of freedom.

His parton cascade description [3] for the early stages of relativistic heavy ion collisions has become very important for our understanding of the experimental

results gathered at the SPS at CERN [4,5]. It will be crucial to the interpretation of data which will be collected at the STAR detector at RHIC [6,7].

RHIC will begin operation in 1999 with four detectors: two medium scale ones, BRAHMS and PHOBOS, as well as two large scale detectors, PHENIX and STAR. The main emphasis of the STAR (Solenoidal Tracker At RHIC) detector will be the correlation of many (predominantly hadronic) observables on an event-by-event basis.

The great energy range and beam target range accessible with RHIC will allow a dedicated systematic search for the quark-gluon phase matter at energy densities an order of magnitude above the transition domain. This occurs not only because the rapidity density of hadrons is expected to be 2–4 times larger than in central SPS collision, but also because pQCD dominated mini-jet initial conditions are finally reached in the collider ($\sqrt{s} \sim 200$ AGeV) energy range. A whole class of new signatures involving hard pQCD probes (high $p_{\rm t}$ and jets) becomes available.

At yet higher energies at LHC, quark-gluon plasma research efforts and planning are centered around the ALICE detector. Its design is similar to that of STAR. ALICE will be the only large scale heavy ion detector setup at LHC. At $\sqrt{s} \sim 5$ ATeV even bottom quarkonia are copiously produced and transverse momenta twice as high ($p_{\rm t} \sim 60$ GeV/c) will be readily measurable to probe even deeper into the multiparticle dynamics of a QGP.

CRITICAL REVIEW OF QGP SIGNATURES

In the last few years researchers at Brookhaven and CERN have succeeded to measure a wide spectrum of observables with heavy ion beams, Au+Au and Pb+Pb. While these programs continue to measure with greater precision the beam energy–, nuclear size–, and centrality dependence of those observables, it is important to recognize the major milestones for relativistic heavy ion physics passed thus far in that work.

The experiments have conclusively demonstrated the existence of strong nuclear A dependence of, among others, J/ψ and ψ' meson production and suppression, strangeness enhancement, hadronic resonance production, stopping and directed collective transverse and longitudinal flow of baryons and mesons – in and out of the impact plane, both at AGS and SPS energies –, and dilepton-enhancement below and above the ρ meson mass. These observations support that a novel form of "resonance matter" at high energy- and baryon density has been created in nuclear collisions. The global multiplicity and transverse energy measurements prove that substantially more entropy is produced in $A + A$ collisions at the SPS than simple superposition of $A \times pp$ would imply. Multiple initial and final state interactions play a critical role in all observables. The high midrapidity baryon density (stopping) and the observed collective transverse and directed flow patterns constitute one of the strongest evidence for the existence of an extended period ($\Delta\tau \approx 10$ fm/c) of high pressure and strong final state interactions. The enhanced ψ' suppression in

$S+U$ relative to $p+A$ also attests to this fact. The anomalous low mass dilepton enhancement shows that substantial in-medium modifications of multiple collision dynamics exists, probably related to in-medium collisional broadening of vector mesons. The non-saturation of the strangeness (and anti-strangeness) production shows that novel non-equilibrium production processes arise in these reactions. Finally, the centrality dependence of J/ψ absorption in $Pb+Pb$ collisions presents further hints towards the nonequilibrium nature of such reactions. Is there evidence for the long sought-after quark-gluon plasma that thus far has only existed as a binary array of predictions inside teraflop computers?

As we will discuss, it is too early to tell. Theoretically there are still too many "scenarios" and idealizations to provide a satisfactory answer. Recent results from microscopic transport models as well as macroscopic hydrodynamical calculations differ significantly from predictions of simple thermal models, e. g. in the flow pattern. Still, these nonequilibrium models provide reasonable predictions for the experimental data. We may therefore be forced to rethink our concept of what constitutes the deconfined phase in ultrarelativistic heavy-ion collisions. Most probably it is not a blob of thermalized quarks and gluons. Hence, a quark-gluon plasma can only be the source of *differences* to the predictions of these models for hadron ratios, the J/Ψ meson production, dilepton yields, or the excitation function of transverse flow. And there are experimental gaps such as the lack of intermediate mass $A \approx 100$ data and the limited number of beam energies studied thus far, in particular between the AGS and SPS.

In the future, the field is at the doorstep of the next milestone: $A+A$ at $\sqrt{s} = 30-200$ AGeV are due to begin at RHIC/BNL in the summer of 1999, and at even higher energies ($\sqrt{s} < 5$ ATeV) at LHC/CERN in the next millennium.

Here, the results of Klaus Kinder-Geiger are of great importance for an understanding of the data to come: Any theoretical description of the early stages of events observed with these machines, reaching extremely high energy and matter densities, must take care of the partonic degrees of freedom (see [4], and Fig. 1). One way of doing this is the use of parton cascade models, as initiated and furthered by Klaus.

NONEQUILIBRIUM MODELS

In the present survey of relativistic heavy ion collisions, we employ two sharply distinct nonequilibrium models, namely the macroscopic 3-fluid hydrodynamical model [8] and the Ultra-relativistic Quantum Molecular Dynamical model, UrQMD [9]. The first model assumes that a projectile- and a target fluid interpenetrate upon impact of the two nuclei, creating a third fluid (in the present version baryon free, see, however, [10]) via new source terms in the continuity equations for energy- and momentum flux. Those source terms are taken from energy- and rapidity loss measurements in high energy pp-collisions. The equation of state (EoS) of this model assumes equilibrium only in each fluid separately and allows for a first order

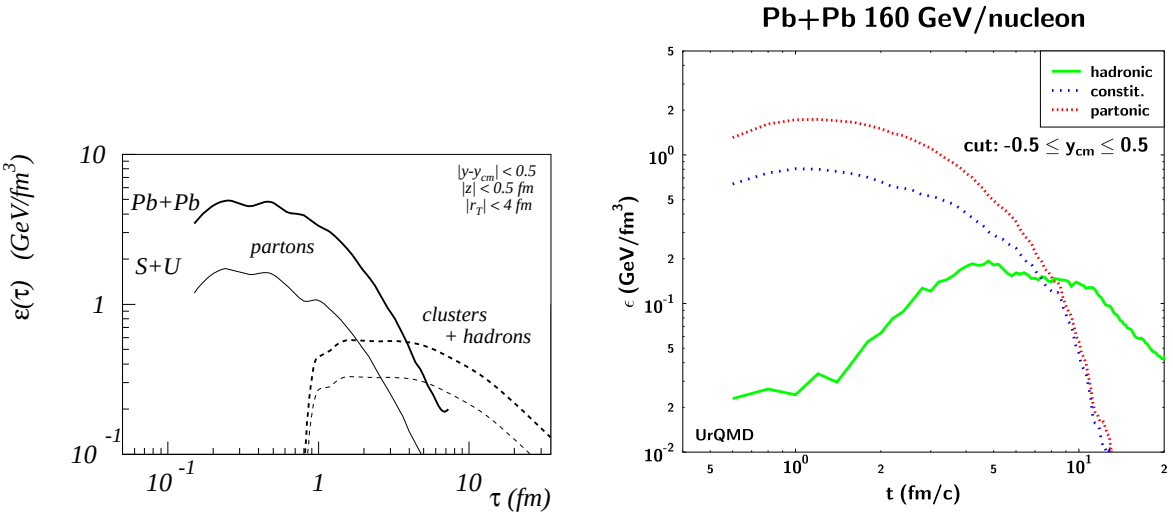

FIGURE 1. (Left) Klaus Kinder-Geigers parton cascade (VNI, from [4]) and (Right) UrQMD results for the time evolution of energy density in central $Pb + Pb$ reactions at 160 AGeV. At an early stage, most of the energy is contained in the partonic degrees of freedom (VNI) or in constituents (UrQMD).

phase transition to a quark gluon plasma in fluid 1, 2 or 3, if the energy density in the fluid under consideration exceeds the critical value for two phase coexistence. Pure QGP can also be formed in every fluid separately, if the energy density in that fluid exceeds the maximum energy density for the mixed phase. The UrQMD model, on the other hand, assumes an independent evolution of hadrons, strings, and constituent quarks and diquarks in a nonequilibrium multiparticle system. The collision terms in this system of coupled Boltzmann (partial differential-/integral-) equations are taken from experimental data, where available, and otherwise from additive quark model and string phenomenology.

What is the role of partonic degrees of freedom in relativistic heavy ion reactions at the SPS?

Fig. 1 shows the time evolution of the energy density ϵ in central $Pb+Pb$ reactions at 160 AGeV as obtained within *a)* the parton cascade approach VNI [4] of Klaus Kinder-Geiger, *b)* the UrQMD model [11]. It can be seen that in both models and at early times of the collision, a large fraction of the energy density is contained in partonic degrees of freedom (VNI) or to nearly equal parts in constituent diquarks and quarks from the strings and in virtual hadrons. This (virtual) "partonic" phase in $Pb + Pb$ reactions at 160 AGeV is, however, not to be identified with an equilibrated QGP. Note that the absolute values differ by a factor 2 in the two models and depend heavily on the rapidity cuts imposed to discriminate between virtual free streaming and interacting matter.

While there is currently a strong debate whether (equilibrated) deconfined matter may have been produced at the CERN/SPS, it is widely expected that in collisions

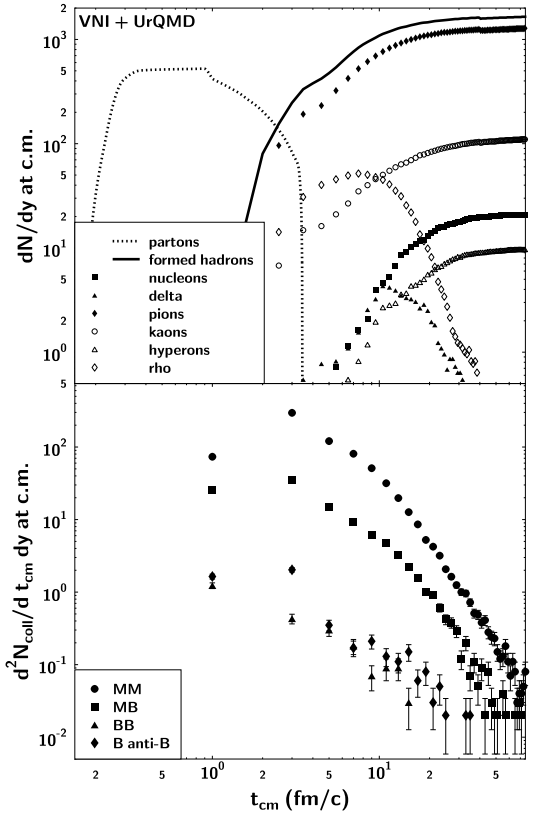

FIGURE 2. (Top) Time evolution of the parton and on-shell hadron rapidity densities at c.m. for central ($b \leq 1$ fm) $Au + Au$ collisions at RHIC. There exists a considerable overlap between the partonic and hadronic phases of the reaction. Hadronic resonances are formed and remain populated up to ≈ 20 fm/c indicating a large amount of hadronic interaction. (Bottom) Rates for hadron-hadron collisions per rapidity at c.m.. Meson-meson and to a lesser extent meson-baryon interactions dominate the dynamics of the hadronic phase.

of heavy nuclei at RHIC a QGP will be formed. The consequence is that at RHIC, both, partonic and hadronic, degrees of freedom have to be treated explicitly. A large step in that direction has been recently undertaken by modeling the initial parton dynamics in the framework of the parton cascade model, performing hadronization via a cluster hadronization model and configuration space coalescence, and finally describing the hadronic phase either by a hadronic after-burner [6] or by a full microscopic hadronic transport approach [12]. Technically the latter approach is realized by combining VNI [4] for the initial phase and hadronization with UrQMD [9] for the later, hadronic, reaction stages. The resulting reaction dynamics indicates a strong influence of hadronic rescattering on the space-time pattern of hadronic freeze-out and on the shape of transverse mass spectra. The upper frame of figure 2 shows the time evolution (in c.m. time, $t_{c.m.}$) of the rapidity density dN/dy of partons (i.e. quarks and gluons) and on-shell hadron multiplici-

ties at $|y_{c.m.}| \leq 0.5$. Note that there are no distinctly separate time scales for the three reactions stages discussed earlier in this article: hadronic and partonic phases may evolve in parallel and both, parton-parton as well as hadron-hadron interactions occur in the same space-time volume. The overlap between the partonic and hadronic stages of the reaction stretches from $t_{c.m.} \approx 1$ fm/c up to $t_{c.m.} \approx 4$ fm/c for the midrapidity region. The calculation indicates that this overlap occurs not only in time but also in coordinate space – partonic and hadronic degrees of freedom occupy the same space-time volume during this reaction phase [12]. Hadronic resonances like the $\Delta(1232)$ and the $\rho(770)$ (which are the most abundantly produced baryonic and mesonic resonance states) are formed and remain populated up to $t_{c.m.} \approx 15 - 20$ fm/c, indicating a considerable amount of hadronic rescattering. Hadron yields saturate at time-scales $t_{c.m.} \approx 25$ fm/c. Since resonance decays have not been factored into this estimate of the saturation time, this number should be viewed as an upper estimate for the time of chemical freeze-out.

Rates for hadron-hadron collisions per unit rapidity at $y_{c.m.}$ are shown in the lower frame of figure 2, i.e. all hadron-hadron collisions for hadrons with $|y_{c.m.}| \leq 0.5$ were taken into account. Meson-meson and meson-baryon interactions dominate the dynamics of the hadronic phase. Due to their larger cross sections baryon-antibaryon collisions occur more frequently than baryon-baryon interactions. However, both are suppressed as compared to meson-meson and meson-baryon interactions. This is due to the large meson multiplicity, which creates a "mesonic medium" in which the baryons propagate.

A comparison of calculations with and without hadronic rescattering shows that e.g. the proton and antiproton multiplicities change by a factor of two due to hadronic rescattering, whereas the ratio of their yields remains roughly constant. Evidently chemical freeze-out of the system occurs well into the hadronic phase and not at the "phase-boundary". The collision rates indicate that interactions cease at $t_{c.m.} \approx 30 - 40$ fm/c at which point the system can be regarded as kinetically frozen out. Since the saturation of the hadron yields occurs earlier, there is a clear separation between chemical and kinetic freeze-out.

YIELDS OF HADRONIC PROBES

Let us now discuss the results obtained from hadronic probes, such as observed production of J/Ψ mesons, enhancement of strange baryons, light mesons, and particle ratios. Observed hadrons include feeding by the decay of resonances.

J/ψ suppression

Debye screening of heavy charmonium mesons in an equilibrated quark-gluon plasma may reduce the range of the attractive force between heavy quarks and antiquarks [13]. Mott transitions then dissolve particular bound states, one by one. NA38 found evidence of charmonium suppression in light ion reactions. Then also

$c\bar{c}/b\bar{b}$-state	J/Ψ	Ψ′	χ_{c10}	χ_{c11}
$< b^2 >$ (fm^2)	0.094	0.385	0.147	0.293
$\sigma_{\rm nonperturbative}$ (mb)	3.62	20.0	6.82	15.9
$\sigma_{\rm hard}$ (mb) (SPS)	0.024	0.012	0.021	0.006
$\sigma_{\rm hard}$ (mb) (RHIC)	1.73	0.68	1.23	0.30
$\sigma_{\rm hard}$ (mb) (LHC)	20.8	8.2	14.7	3.5

TABLE 1. The average square of the transverse distances of the charmonium states and the total quarkonium-nucleon cross sections σ. For the χ two values arise, due to the spin dependent wave functions ($lm = 10, 11$). $\sigma_{\rm hard}$ are the perturbative QCD contribution at different energies.

in $p + A$ such suppression was observed. New preliminary $Pb + Pb$ data of NA50 show "anomalous" suppression.

One of the main problems in the interpretation of the observed suppression as a signal for deconfinement is that non-equilibrium dynamical sources of charmonium suppression have also been clearly discovered in $p+A$ reactions, where the formation of an equilibrated quark-gluon plasma is not expected. A recent development is the calculation of the hard contributions to the charmonium- and bottonium-nucleon cross sections based on the QCD factorization theorem and the non-relativistic quarkonium model [14]. Including non-perturbative contributions, the calculated $p + A$ cross section agrees well with the data.

The numerical calculation shown in Tab. 1 was done for charmonium states produced in midrapidity at SPS energy and in the target fragmentation region at RHIC and LHC. One can see that the hard contribution to the cross section is just a correction at SPS energies, but at RHIC energies both contributions become comparable and at LHC it dominates (one neglects here that the DGLAP equation (Dokshitser-Gribov-Lipatov-Altarelli-Parisi) should be probably violated [20]).

Whereas these descriptions of nuclear absorption can account for the $p+A$ observation, the corrections needed for an extrapolation to $A+A$ reactions are, however, not yet under theoretical control.

Purely hadronic dissociation scenarios have been suggested [15–17] which could account for J/ψ and ψ' suppression without invoking the concept of deconfinement ("comover models"). Suppression in excess to that due to preformation and nuclear absorption is ascribed in such models to interactions of the charmonium mesons with "comoving", but probably off-equilibrium, mesons and baryons, which are produced copiously in nuclear collisions. Fig. 3 shows an UrQMD calculation which employs a microscopic free streaming simulation for J/ψ production and a microscopic transport calculation for nuclear and comover dynamics as well as for rescattering [19]. The dissociation cross sections are calculated using the QCD factorization theorem [14], feeding from ψ' and χ states is taken into ac-

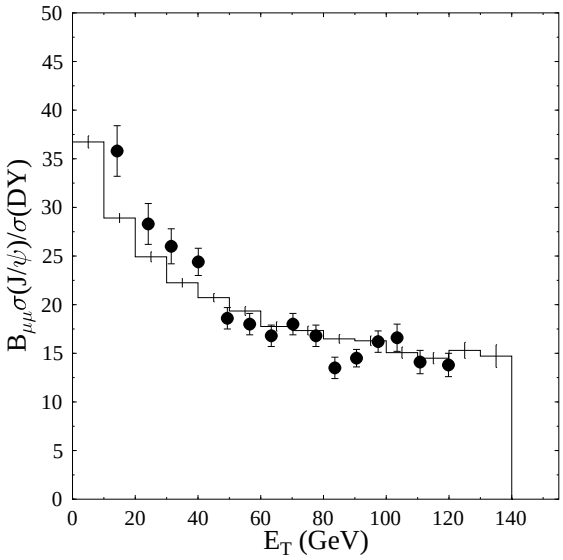

FIGURE 3. The ratio of J/ψ to Drell-Yan production as a function of $E_{\rm t}$ for $Pb+Pb$ at 160 GeV. The experimental data are from Ref. [18], the histogram is a UrQMD calculation [19]. No scaling factor has been applied to the x-axis for either the calculations or the data.

count, and the $c\bar{c}$ dissociation cross sections increase linearly with time during the formation of the charmonium state. Taking into account the non-equilibrium "comovers" ($\sigma_{\rm meson} \approx 2/3\sigma_{\rm nucleon}$), the agreement between theory and data is reasonable (Fig. 3). New, unpublished data agree better with the model predictions, but the high and low $E_{\rm t}$ regions remain to be studied carefully in the experiment. At present, no ab initio calculation does predict sudden changes in the suppression. In fact, from three-fluid calculations, even with QGP phase included, only a moderate change of the average and local energy density with bombarding energy is predicted. This seems to strongly speak against drastic threshold effects in the charmonium production.

The strong dependence of these results on details, such as the treatment of the formation time or the time dependent dissociation cross section, remain to be studied further. Furthermore, quantum effects such as energy dependent formation and coherence lengths must be taken into account [21] before definite statements can be made with regard to the nature of the J/ψ suppression. Interpretations of the data based on plasma scenarios are also increasingly evolving away from the original Mott transition analog [22,23].

Hence, the theoretical debate on the interpretation of the pattern of charmonium suppression discovered by NA38/NA50 at the SPS is far from settled. It is not clear whether the suppression is the smoking gun of nonequilibrium dynamics or deconfinement. It is not likely to be due to simple Debye screening.

The major goal of further theoretical work is not to continue to try to rule out more "conventional" explanations, but to give positive proof of additional suppres-

sion by QCD-calculations which actually *predict* the E_t-dependence of the conjectured signature. Consistency tests and a detailed simultaneous analysis of all other measured observables are needed, if at least the same standards as for the present calculations are to be hold up.

Particle ratios

The study of particle ratios has recently attended great interest at the AGS [24–26] and at the SPS [27,28].

One assumes a thermalized system with a constant density $\rho(r)$ (box profile), a constant temperature $T(r)$ and a linear radial and longitudinal flow velocity profile $\beta_\perp(r)$, $\beta_{||}(r)$. These parameters are assumed to be the same for all hadrons/fragments. At some time $t^{\rm break-up}$ and density $\rho^{\rm break-up}$, the system decouples as a whole (a horizontal freeze-out in the $T(z)$-plane) and the particles are emitted instantaneously from the whole volume of the thermal source. A complete loss of memory results, due to thermalization – the emitted particles carry no information about the evolution of the source. If one wants to use the inverse slope parameter T as thermometer [29], the feeding from Δ's etc., as well as the radial flow need to be incorporated into the analysis. The same holds for the use of d/p, π/p etc. as an entropymeter [30]. In addition, the proper Hagedorn volume correction can be applied [31]. A two parameter fit ($\mu_{\rm q}$, T, $\mu_{\rm s}$ is fixed by strangeness conservation) to the hadronic freeze-out data describes the experimental results well, if feeding is included [28]. Does this compatibility with a thermal source proof volume emission from a globally equilibrated source?

The ideal gas thermal fit to experimental data for hadron ratios in $S + Au$ collisions at 200 AGeV gives values for the parameters T and $\mu_{\rm B}$ which can be used as input for a $SU(3)$ chiral mean-field model [32] extended to finite temperatures [33]. Feeding from the decay of higher resonances is included. One finds that in such a model (which selfconsistently contains a chiral phase transition at $T \approx 150$ MeV) the ideal gas model values $T = 160$ MeV and $\mu_{\rm B} = 170$ MeV lead to strong deviations from the experimental data. Only the Ω/Ξ^--ratio is in a good agreement, in contrast to the ideal gas model. Hence, the system can not be close to the chiral phase transition – the T and μ values extracted from the free thermal model cannot be identified with the real temperature and chemical potential of the system!

The chiral mean-field model does reproduce the data compiled in [34] for relative abundances in $Pb + Pb$ collisions at 160 AGeV (Fig. 4, left) for $T = 125$ MeV and $\mu_B = 180$, much lower than the thermal model results [35,34] ($T = 160 - 175$ MeV, $\mu_{\rm B} = 200 - 270$ MeV). The microscopic UrQMD transport model is in good agreement with the measured hadron ratios of the system $S + Au$ at CERN/SPS [36]. A thermal model fit to the calculated ratios yields a temperature of $T = 145$ MeV and a chemical potential of $\mu_{\rm B} = 165$ MeV. However, these ratios exhibit a strong rapidity dependence. Thus, thermal model fits to data may be distorted due to different acceptances for the individual ratios.

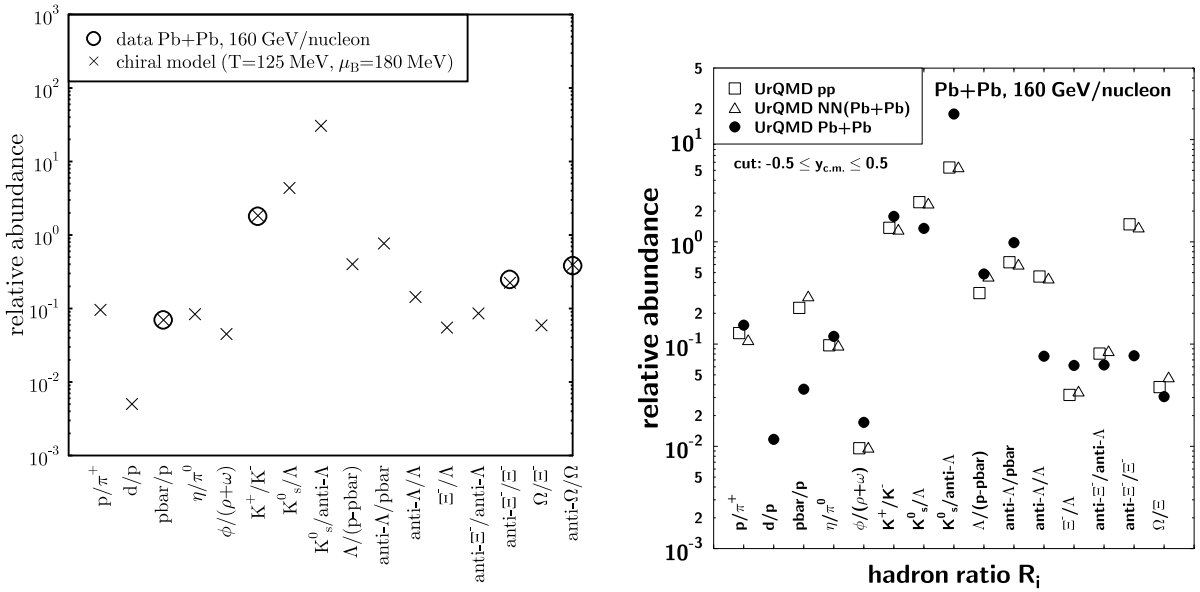

FIGURE 4. (Left) Fit of hadron ratios from the chiral model to preliminary data from $Pb+Pb$ collisions at SPS. The obtained values of T and μ allow the prediction of further ratios. T and μ are much lower than thermal model results from the ideal hadron gas . (Right) UrQMD prediction for hadron ratios in $Pb+Pb$ collisions at midrapidity (full circles), compared to a superposition of pp, pn and nn reactions with the isospin weight of the $Pb+Pb$ system (open triangles), i.e. a first collision approach.

Hadron ratios for the system $Pb+Pb$ are predicted by UrQMD and can be fitted by a thermal model with $T = 140$ MeV and $\mu_B = 210$ MeV (Fig. 4, right). Analyzing the results of non-equilibrium transport model calculations by an equilibrium model may, however, be not meaningful.

There is a problem in the definition of equilibrium in itself: Do heavy ion collisions ever reach a thermalized system? Or are there transient steady states off equilibrium [37]? Due to the rapid dynamics of the system, the assumption of detailed balance is not fulfilled in the initial stage. This drives the system into a steady state far from equilibrium, but stationary in time. This steady state is easily visible in an enhanced production of light mesons, as compared to thermal models.

During the initial off-equilibrium stage of energetic nuclear collisions, a large amount of entropy can be produced [38]. The subsequent expansion is, on the other hand, often assumed to be nearly isentropic. The entropy produced during the compression stage is closely linked to the finally observable relative particle yields.

This entropy production can be calculated [39] within three-fluid hydrodynamics. The entropy per net participating baryon, S/A, saturates rapidly as a function of CM-time and is essentially time independent for later times when the freeze-out

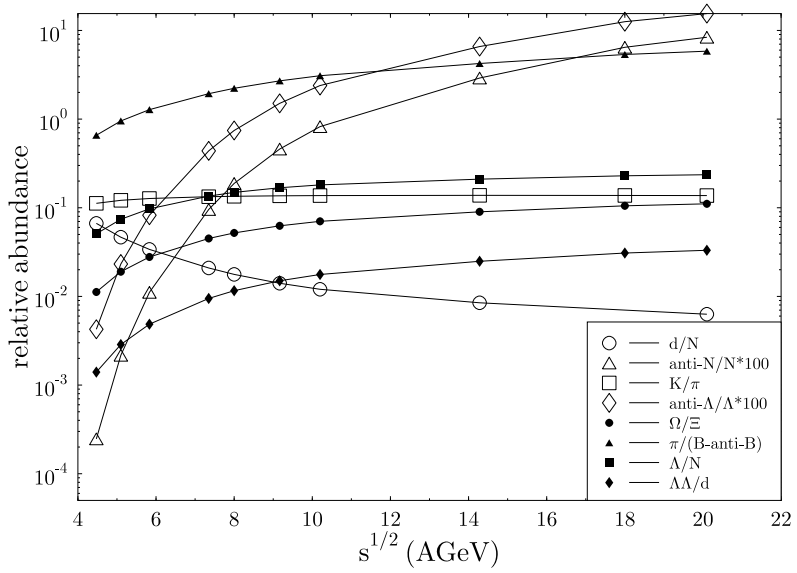

FIGURE 5. The excitation function of various particle ratios as calculated from the S/A values obtained from the three-fluid model. Feeding due to decays of resonances is taken into account.

is reached. The chemical composition of the fireball is given by the net baryon density, the net (zero) strangeness of the system, and the specific entropy S/A, as described for the thermal model above.

The hadron ratios thus obtained are shown in Fig. 5. At AGS and SPS energies, they are quite close to the data [27,40]. For such a simple estimate of hadron production in nuclear collisions, deviations from the experimental ratios by up to factors of two have to be expected. Nevertheless, it is clear from Fig. 5 that the simultaneous measurement of various hadron ratios, like $\pi/\left(B-\overline{B}\right)$, d/$N$ and, in particular, $\overline{B}/B$ (provided antibaryons also reach chemical equilibrium) allows to determine the produced entropy in the energy range between the AGS and the SPS. In contrast, the K/π-ratio is practically constant. The total specific entropy S/A produced within the three-fluid model is consistent with the S/A values extracted from data using relative particle yields from the thermal model. One finds $S/A = 11$ for AGS and $S/A = 38$ for SPS energies.

The excitation function of the specific entropy $S/A(\sqrt{s})$ does not exhibit any threshold signatures of the phase transition to the QGP incorporated in the EoS. This is due to the gradual transition through the wide coexistence region in the energy density between $E_{\rm lab} \approx$ 10–100 AGeV.

Strange baryons and mesons, Hypermatter and Strangelets

Let us now turn to multi-strange signals. In nucleon nucleon collisions, the production of particles containing strange quarks is strongly suppressed as compared

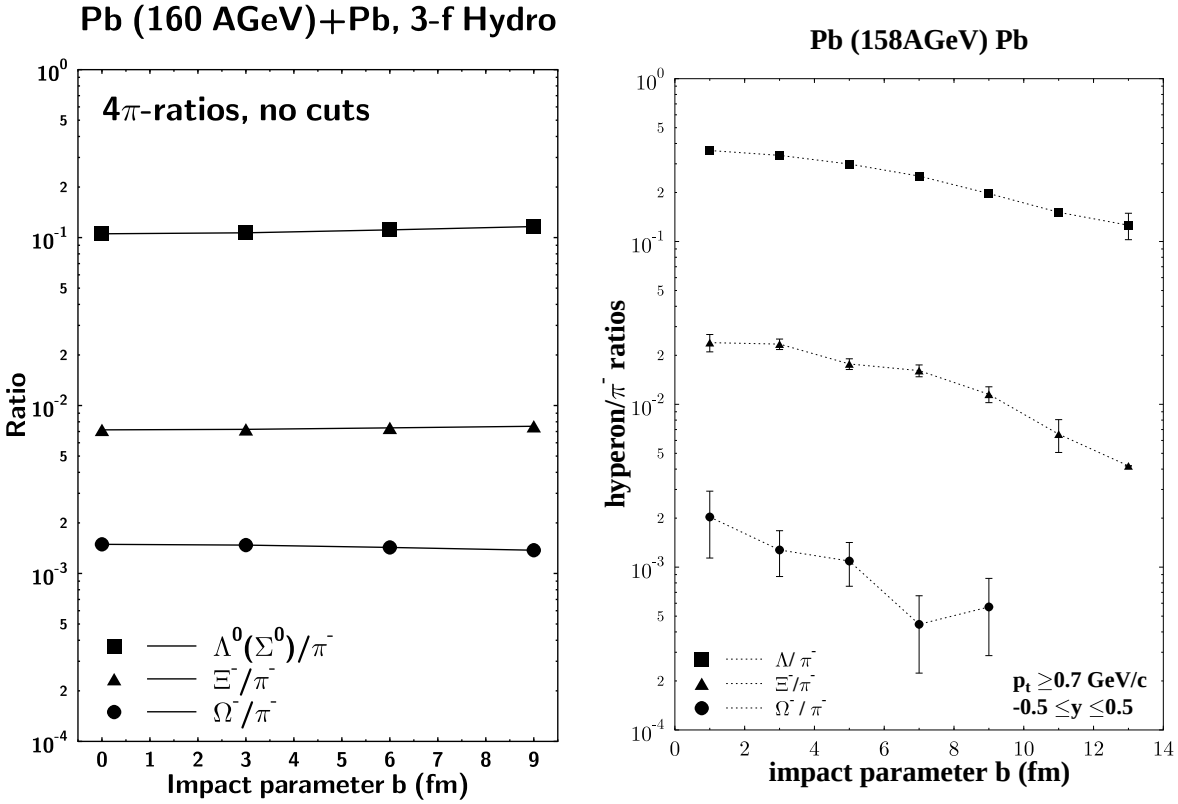

FIGURE 6. Hyperon to π^- ratio as a function of impact parameter b, as obtained from the three-fluid hydrodynamical model (Left) and the UrQMD model (Right). In the UrQMD model, the observed strangeness enhancement is already a natural consequence of ordinary hadronic rescattering.

to the production of particles with u and d quarks due to the higher mass of the $s\bar{s}$ quark pair.

It has been speculated that the yield of strange and multi-strange mesons, (anti-) baryons and anti-hyperons ($\bar{\Lambda}, \bar{\Sigma}, \bar{\Xi}$ and $\bar{\Omega}$) should be enhanced in the presence of a QGP.

The study of (multi)strange hyperons by the WA97 [41] and the NA49 collaborations show an enhancement of strangeness production for central collisions when studying the centrality dependence of various strange particle yields (Λ, Ξ, Ω) in $Pb+Pb$ collisions at 158 AGeV as compared to $p+Pb$ collisions at 158 AGeV. The centrality is given as the extrapolated number of participant nucleons $N_{\rm part}$. We propose as centrality variable the number of produced pions N_{π^-}. $N_{\rm part}$ shows a nonlinear behavior with the volume of the participant zone, while N_{π^-} shows perfect participant scaling. Scaling has been observed for central collisions ($N_{\rm part} \geq 100$).

The UrQMD calculations (Fig. 6, right) show scaling. The hyperon to π^- ratio is depicted in Fig. 6 (Right) as a function of impact parameter b. For central

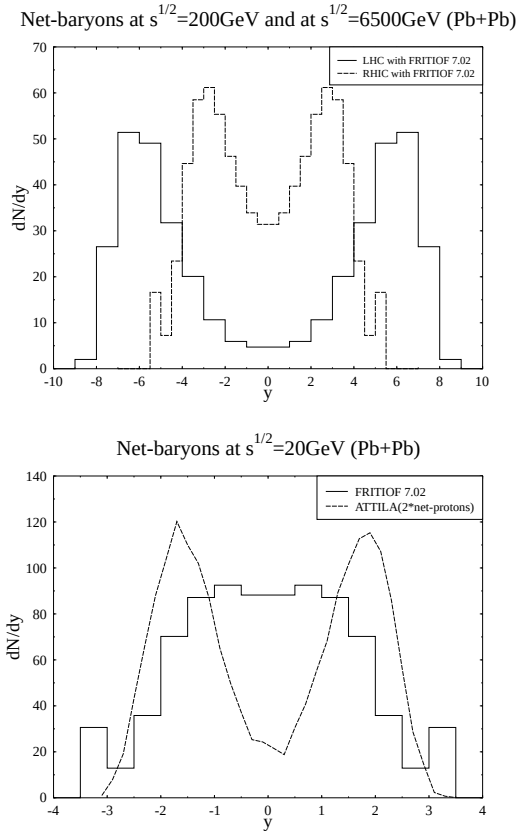

FIGURE 7. Net-baryon rapidity distribution of very central $Pb+Pb$ collisions at SPS, RHIC, LHC calculated with FRITIOF 7.02. The midrapidity region is even at LHC not net-baryon-free. For comparison the net-protons at SPS calculated with ATTILA are also shown.

collisions, all ratios change only moderately, thus an approximate linear scaling of the hyperon yield with pion number N_{π^-} is observed. For peripheral collisions, the ratios decrease. The ratios vary with a factor of 2 to 5 for different impact parameters depending on the hyperon and its strangeness content. The three-fluid hydrodynamical model with an EoS with a first order phase transition to a QGP yields constant ratios (Fig. 6 left). Note the substantial differences in the Ξ/π-ratios between the two predictions. A comparison to upcoming data by the NA49 and CERES may provide an estimate of the degree of local chemical equilibration.

Fig. 7 exhibits the baryon rapidity distribution as predicted by various models for heavy ion collisions. ATTILA [42] and FRITIOF 1.7 [43] (not in the picture) show nearly a baryon-free midrapidity region already at SPS(CERN). These models are therefore ruled out by the new CERN data, which rather support predictions based on the RQMD model [44]. Also the new Lund model release FRITIOF 7.02 yields stopping at SPS! At RHIC, FRITIOF 7.02 and RQMD [45] predict that the

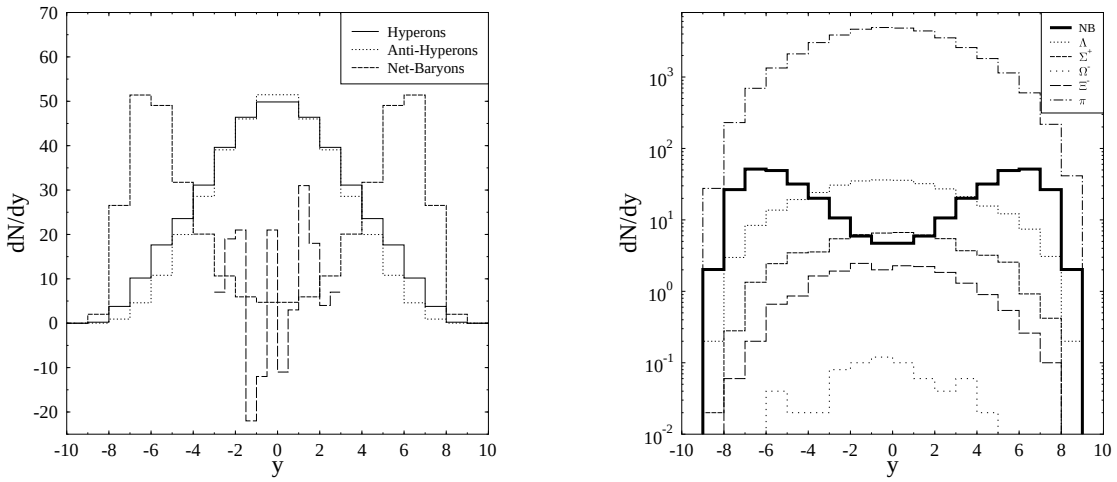

FIGURE 8. (Left) The (anti-)hyperon rapidity distribution and mean net-baryon distribution at midrapidity compared with the distribution of a single event, and (Right) Rapidity distributions of different particles (NB denotes net baryons), both in very central $Pb + Pb$ collisions at $\sqrt{s}_{NN} = 6.5$ TeV, calculated with FRITIOF 7.02.

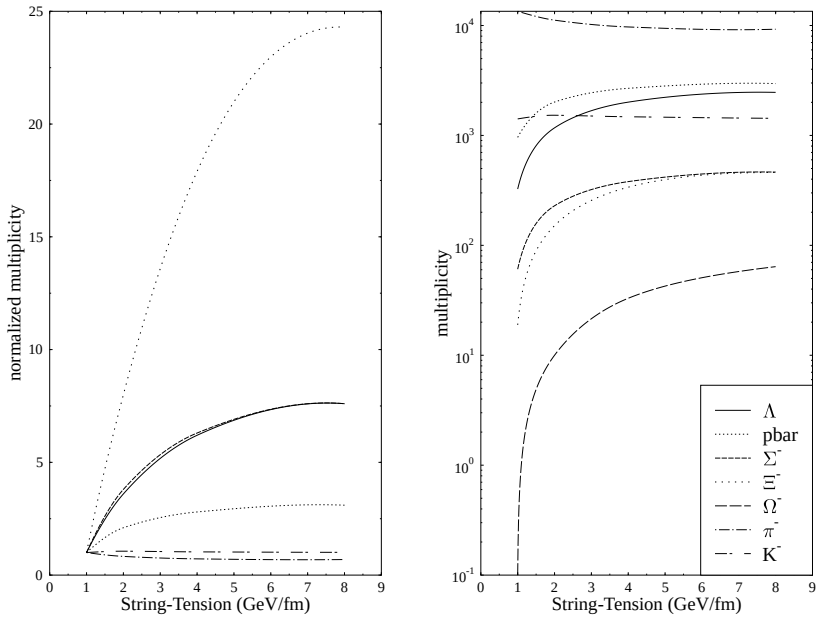

FIGURE 9. The multiplicities of different particles in very central $Pb + Pb$ collisions at LHC calculated with FRITIOF 7.02 as function of the string-tension.

net baryon number $A \gg 0$ at $y_{\rm cm}$. Furthermore, even in very central collisions of lead on lead at $\sqrt{s}_{NN} = 6.5$ TeV, there might be some net-baryon density at midrapidity. This is shown in Fig. 8 (Left), where the event-averaged rapidity densities of net-baryons, hyperons and anti-hyperons are depicted for LHC, using FRITIOF 7.02. If this non-perfect transparency turns out to be true, the finite baryo-chemical potential at midrapidity may have strong impact on the further evolution of the system. Expected yields of strangelets will be extremely sensitive to the initial baryon-number of a Quark-Gluon-Plasma-phase.

Fig. 8 (Right) shows the event-averaged rapidity densities of net-baryons, hyperons and pions calculated with FRITIOF 7.02. Note that the strange to non-strange hadron ratios predicted by this model are the same for pp and AA collisions at 200 AGeV/c (CERN-SPS) and that the strange particle numbers for AA underpredict the data [46]. This deficient treatment of the collective effects in the model leads us to take the numbers only as lower limits of the true strange particle yields at collider energies.

Keep in mind that the microscopic models used here ignore possible effects that could change significantly the number of produced strange particles in heavy ion collisions, e.g. string-string-interactions. An enhanced string tension may effectively simulate string-string interaction, as shown in Fig. 9. Here the multiplicities of different produced particles at LHC as function of the string-tension κ are depicted. A higher string-tension, e.g. 2 GeV/fm yields the suppression factors u : d : s : qq = 1 : 1 : 0.55 : 0.32.

DILEPTON PRODUCTION

Besides results from hadronic probes, electromagnetic radiation – and in particular dileptons – offer an unique probe from the hot and dense reaction zone: here, hadronic matter is almost transparent. The observed enhancement of the dilepton yield at intermediate invariant masses ($M_{e^+e^-} > 0.3$ GeV) received great interest: it was prematurely thought that the lowering of vector meson masses is required by chiral symmetry restoration (see e.g. [47] for a review). However, there seems no theoretical support for this speculation. Calculations within a chiral $SU(3)$ mean-field approach [32] show only a modest dependence of temperature of the mass of the ρ meson (Fig. 11, right). AA-data are compatible with broadening spectral functions found in pure hadronic calculations of the scattering on the constituents of the excited matter (see e.g. [48]). The present data do not allow to draw definite conclusions.

Fig. 10 shows a microscopic UrQMD calculation of the dilepton production in the kinematic acceptance region of the CERES detector for $Pb + Au$ collisions at 158 GeV. This is compared with the '96 CERES data [49]. Aside from the difference at $M \approx 0.4$ GeV there is a strong enhancement at higher invariant masses. It is expected that this discrepancy at $m > 1$ GeV could be filled up by direct dilepton production in meson-meson collisions [50] as well as by the mechanism of secondary

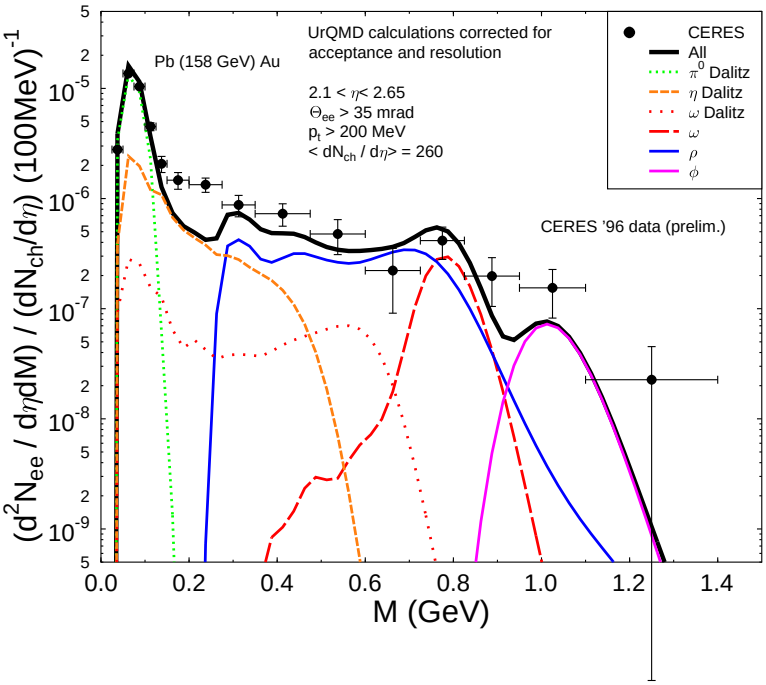

FIGURE 10. Microscopic calculation of the dilepton production in the kinematic acceptance region of the CERES detector for $Pb + Au$ collisions at 158 GeV. No in-medium effects are taken into account. Plotted data points are taken at CERES in '96.

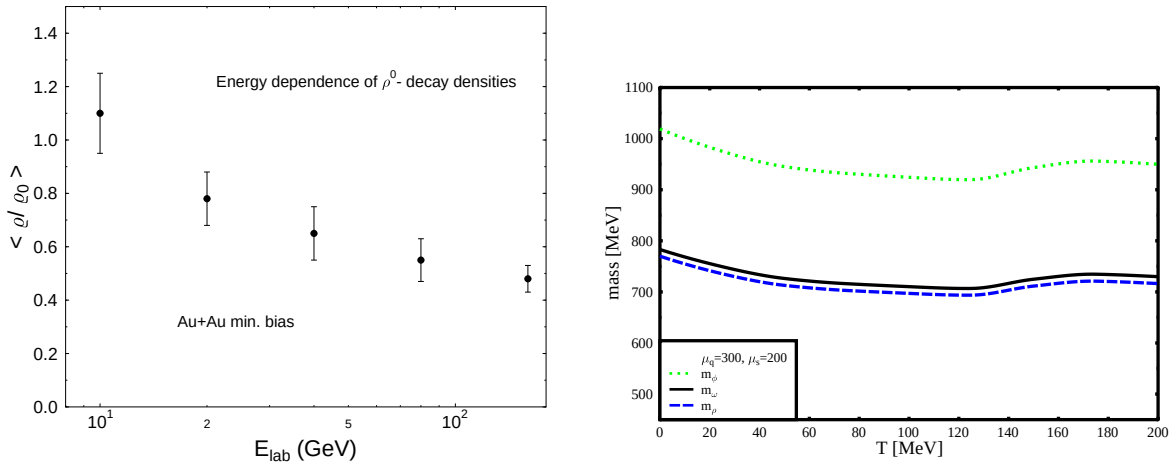

FIGURE 11. (Left) The mean "freeze-out" density at the location of ρ meson decays in $Au + Au$ collisions. (Right) The mass of the ρ-meson as obtained from the chiral model at different temperatures and finite density.

Drell-Yan pair production proposed in [51].

The mean "freeze-out" density at the location of ρ meson decays in $Au + Au$ collisions is shown in Fig. 11 (Left) for different incident energies [52]. From AGS to CERN energies, there is a decrease of the baryonic density, indicating that baryonic modifications to the ρ meson are better studied at energies of $20 - 40$ AGeV. The low baryon densities at high energies will make it hard to explain the CERES data by ρ meson modifications of nucleonic origin alone.

COLLECTIVE FLOW AND THE SOFTENING OF THE EOS

The excitation function of collective transverse flow is the earliest predicted signature for probing compressed nuclear matter. Transverse collective flow depends directly on the pressure $p(\rho, S)$, i.e. the EoS. The flow excitation function is sensitive to phase transitions [29] by a collapse of the directed transverse flow [53,54]. This is commonly referred to as *softening* of the EoS [55].

An observation of a local minimum in the excitation function of the transverse directed flow would thus be an unambiguous signal for a first order phase transition in dense matter. It's experimental measurement would serve as strong evidence for a QGP, if that phase transition is of first order.

Recent calculations within three-fluid hydrodynamics [56] show a shift in the drop of transverse flow to higher energies, $E_{\rm lab} \approx 20$ AGeV, see Fig. 12. Experimentally,

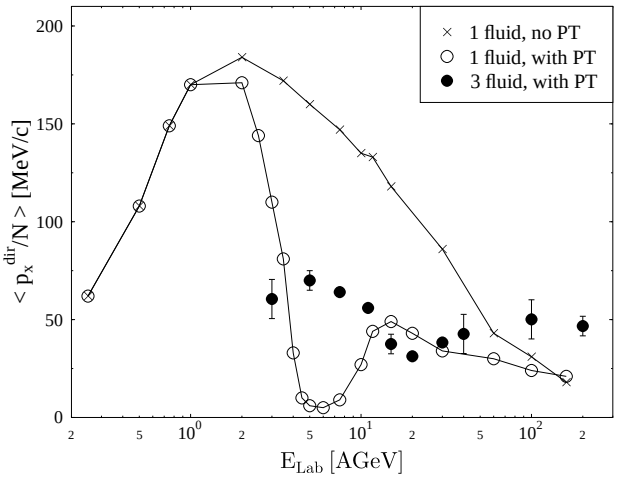

FIGURE 12. The excitation function of transverse flow as obtained from one fluid hydrodynamics with (open circles) and without (crosses) a first order phase transition [55], and the results of the three-fluid hydrodynamical model (filled circles). The drop of p_x due to the softening of the EoS is shifted to $E_{\rm lab} \approx 20$ AGeV.

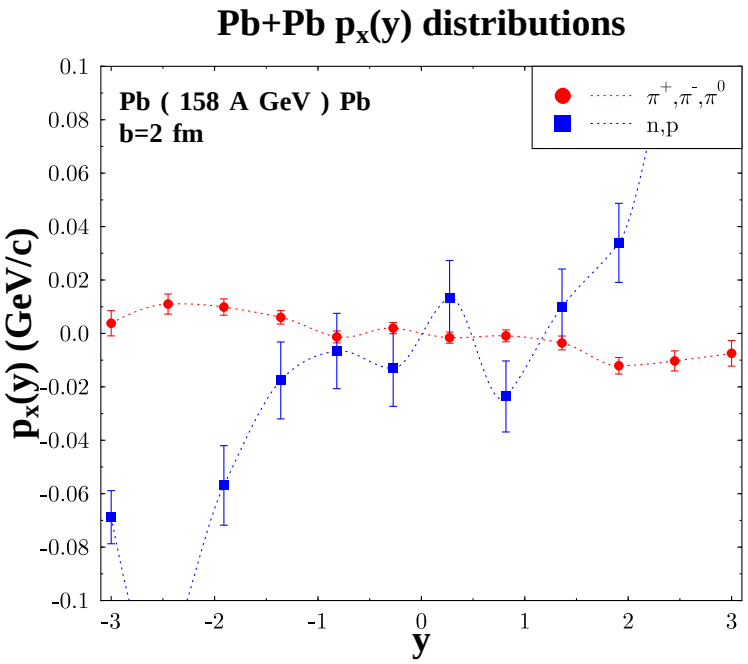

FIGURE 13. Theoretical predictions for transverse collective flow in $Pb + Pb$ collisions as obtained with the microscopic UrQMD transport model [58].

the recent discovery of proton flow and pion antiflow at the SPS is in line with UrQMD and RQMD predictions (Fig. 13, see [57] and [58]).

OUTLOOK

At the CERN/SPS new data on flow, electro-magnetic probes, strange particle yields (most importantly multistrange (anti-)hyperons) and heavy quarkonia will be interesting to follow closely. Simple energy densities estimated from rapidity distributions and temperatures extracted from particle spectra indicate that initial conditions could be near or just above the domain of deconfinement and chiral symmetry restoration. Still the quest for an *unambiguous* signature remains open.

Directed flow has been discovered – now a flow excitation function, filling the gap between 10 AGeV (AGS) and 160 AGeV (SPS), would be extremely interesting to look for the softening of the QCD equation of state in the coexistence region. The investigation of the physics of high baryon density (e.g. partial restoration of chiral symmetry via properties of vector mesons) is presently not accessible due to the lack of dedicated accelerators in the $10 - 200$ AGeV regime.

However, dedicated accelerators would be mandatory to explore these intriguing effects in the excitation function. It is questionable whether this key program will actually get support at CERN. Also the excitation function of particle yield ratios

$(\pi/\mathrm{p}, \mathrm{d}/\mathrm{p}, \mathrm{K}/\pi ...)$ and, in particular, multistrange (anti-)hyperon yields, can be a sensitive probe of physics changes in the EoS. The search for novel, unexpected forms of $SU(3)$ matter, e.g. *hypermatter*, *strangelets* or even *charmlets* is intriguing. Such exotic QCD multi-meson and multi-baryon configurations would extend the present periodic table of elements into hitherto unexplored dimensions. A strong experimental effort should continue in that direction.

For applications to nuclear collision observables, an extension of the QGP concept to non-equilibrium conditions is required. The popular use of simple fireball models may provide convenient parameterizations of large bodies of data, but they will never provide a convincing proof of new physics. Microscopic transport models are required that can address simultaneously all the observables and account for experimental acceptance and trigger configurations.

Present work in parton cascade dynamics is based largely on analogy to transport phenomena in known abelian QED plasmas. A significant new feature of QCD plasmas is its ultrarelativistic nature and the dominance of (gluon) radiative transport. These greatly complicate the equations. The role of quantum coherence phenomena beyond classical transport theories has only recently been established within idealized models. Much further work will be required in this connection. The outstanding theoretical task will be the development of practical (vs. formal) tools to compute quantum non-equilibrium multiple collision dynamics in QCD.

Experiments and data on ultra-relativistic collisions are essential in order to motivate, guide, and constrain theoretical developments. They provide the only terrestrial probes of non-perturbative aspects of QCD and its dynamical vacuum. The understanding of confinement and chiral symmetry remains one of the key questions at the beginning of the next millennium.

ACKNOWLEDGMENTS

This work was supported by DFG, GSI, BMBF, DAAD, Graduiertenkolleg Theoretische und Experimentelle Schwerionenphysik, the A. v. Humboldt Foundation, and the J. Buchmann Foundation.

This paper is dedicated to our colleague and friend, Klaus Kinder-Geiger. Over the last decade, we have had the great pleasure of sharing frequent, sometimes heated, scientific discussions about the physics and the future of our field with Klaus.

Klaus, Du fehlst uns.

REFERENCES

1. Proceedings of the International Conference *"Structure of Vacuum and Elementary Matter"* (South Africa, Wilderness, March 9-15, 1996), edited by H. Hamilton, H. Stöcker, A. Gallmann.
2. K. Geiger, *Phys. Rev.* **D57** 1895 (1998).

3. K. Geiger, R. Longacre, D. K. Srivastava, nucl-th/9806102
4. K. Geiger, *Nucl. Phys.* **A638** 551c (1998).
5. K. Srivastava, K. Geiger, *Phys. Lett.* **B422** 39 (1998).
6. K. Geiger, R. Longacre, *Heavy Ion Phys.* **8** 41 (1998).
7. H. Wieman et al., *Nucl. Phys.* **A638** 559 (1998)
8. J. Brachmann, A. Dumitru, J.A. Maruhn, H. Stöcker, W. Greiner, D.H. Rischke, *Nucl. Phys.* **A619** 391 (1997).
9. S.A. Bass, M. Belkacem, M. Bleicher, M. Brandstetter, L. Bravina, C. Ernst, L. Gerland, M. Hofmann, S. Hofmann, J. Konopka, G. Mao, L. Neise, S. Soff, C. Spieles, H. Weber, L.A. Winckelmann, H. Stöcker, W. Greiner, C. Hartnack, J. Aichelin, N. Amelin, *Prog. Part. Nucl. Phys.* **41** 225 (1998).
10. A. Rosenhauer, L.P. Csernai, J.A. Maruhn, W. Greiner, *Phys. Scripta* **30** 45 (1984).
11. H. Weber et al., to be published
12. S.A. Bass, M. Hofmann, M. Bleicher, L. Bravina, E. Zabrodin, H. Stöcker and W. Greiner, e-Print Archive: nucl-th/9902055 and submitted.
13. T. Matsui, H. Satz, *Phys. Lett.* **178B** 416 (1986).
14. L. Gerland, L. Frankfurt, M. Strikman, H. Stöcker and W. Greiner, *Phys. Rev. Lett.* **81** 762 (1998).
15. D. Neubauer, K. Sailer, B. Müller, H. Stöcker and W. Greiner, *Mod. Phys. Lett.* **A4** 1627 (1989).
16. S. Gavin, R. Vogt, *Nucl. Phys.* **B345** 104 (1990).
17. S. Gavin, R. Vogt, *Phys. Rev. Lett.* **78** 1006 (1997).
18. A. Romana (NA50 Collab.), in *Proceedings of the XXXIIIrd Rencontres de Moriond*, March 1998, Les Arcs, France.
19. C. Spieles, R. Vogt, L. Gerland, S. A. Bass, M. Bleicher, L. Frankfurt, M. Strikman, H. Stöcker, W. Greiner, hep-ph/9810486
20. FELIX Collaboration (E. Lippmaa et al.), CERN-LHCC-97-45, Aug 1997, 197pp
21. J. Hüfner and B. Kopeliovich, Proceedings of PANIC '96 and e-print: nucl-th/9606010.
22. D. Kharzeev, C. Lourenco, M. Nardi, H. Satz, *Z. Phys.* **C74** 307 (1997).
23. H. Satz, *Nucl. Phys.* **A642** 130 (1998).
24. H. Stöcker, A.A. Ogloblin, W. Greiner, LBL-12971 (1981).
25. J. Cleymanns, H. Satz, *Z. Phys.* **C57** 135 (1993).
26. E. Schnedermann, J. Sollfrank, U. Heinz, *Phys. Rev.* **C48** 2462 (1993).
27. P. Braun-Munzinger, J. Stachel, J.P. Wessels, N. Xu, *Phys. Lett.* **B344** 43 (1995).
28. P. Braun-Munzinger, J. Stachel, J.P. Wessels, N. Xu, *Phys. Lett.* **B365** 1 (1996).
29. H. Stöcker and W. Greiner, *Phys. Rep.* **137** 277 (1986).
30. P. Siemens, J. Kapusta, *Phys. Rev. Lett.* **43** 1486 (1979).
31. M.I. Gorenstein, D.H. Rischke, H. Stöcker, W. Greiner, *J. Phys.* **G19** (1993) L69.
32. P. Papazoglou, D. Zschiesche, S. Schramm, J. Schaffner-Bielich, H. Stöcker, W. Greiner, *Phys. Rev.* **C59** 411 (1999).
33. D. Zschiesche et al., to be published
34. G. D. Yen, M. I. Gorenstein, nucl-th/9808012
35. P. Braun-Munzinger, J. Stachel, *Nucl. Phys.* **A638** 3 (1998).
36. S. Bass, M. Belkacem, M. Brandstetter, M. Bleicher, L. Gerland, J. Konopka,

L. Neise, C. Spieles, S. Soff, H. Weber, H. Stöcker, W. Greiner, *Phys. Rev. Lett.* **81** 4092 (1998).
37. L. Bravina, M. Brandstetter, M.I. Gorenstein, E.E. Zabrodin, M. Belkacem, M. Bleicher, S.A. Bass, C. Ernst, M. Hofmann, S. Soff, H. Stöcker, W. Greiner, Submitted to J. Phys. G, nucl-th/9810036;
E. Zabrodin et al., in preparation.
38. W. Scheid, H. Müller, W. Greiner, *Phys. Rev. Lett.* **32** 741 (1974).
39. M. Reiter, A. Dumitru, J. Brachmann, J.A. Maruhn, H. Stocker, W. Greiner, *Nucl. Phys.* **A643** 99 (1998).
40. L. V. Bravina, M. I. Gorenstein, M. Belkacem, S. A. Bass, M. Bleicher, M. Brandstetter, M. Hofmann, S. Soff, C. Spieles, H. Weber, H. Stöcker, W. Greiner, *Phys. Lett.* **B434** 379 (1998).
41. E. Andersen et al., *Phys. Lett.* **B433** 209 (1998).
42. M. Gyulassy, private communication
43. B. Nilsson-Almqvist, E. Stenlund, *Comput. Phys. Comm.* **43** 387 (1987).
44. H. Sorge, H. Stöcker, W. Greiner, *Ann. Phys. (USA)* **192** (1989) 266; *Nucl. Phys.* **A498** (1989) 567c; *Z. Phys.* **C47** 629 (1990).
45. Th. Schönfeld, H. Stöcker, W. Greiner, H. Sorge, *Mod. Phys. Lett.* **A8** (1993) 2631
46. A. Tai, B. Andersson, Ben-Hao Sa, Proceedings of the International Conference on *"Strangeness in Hadronic Matter"*, S'95, Tucson, AZ, USA, (1995) p.335
47. V. Koch, *Int. Jour. Mod. Phys.* **E6** 203 (1997).
48. W. Cassing, E. L. Bratkovskaya, R. Rapp, and J. Wambach, *Phys. Rev.* C**57** (1998) 916
49. G. Agakishiev et al., *Phys. Lett.* **B402** (1998) 405
50. G. Q. Li and C. Gale, *Phys. Rev.* **C58** 2914 (1998).
51. C. Spieles, H. Stöcker, C. Greiner, *Eur. Phys. J.* **C5** (1998) 349
52. L. A. Winckelmann, PhD thesis, Johann Wolfgang Goethe University, Frankfurt, Germany, 1996.
53. J. Hofmann, H. Stöcker, U. Heinz, W. Scheid, W. Greiner, *Phys. Rev. Lett.* **36** 88 (1976).
54. Ch. Hartnack, H. Stöcker, W. Greiner, Proc. of the Nato Adv. Study Inst. on the Nucl. Equation of State (Peñiscola, Spain), Editors W. Greiner and H. Stöcker, Plenum Press (1990).
55. D. H. Rischke, Y. Pürsün, J.A. Maruhn, H. Stöcker, W. Greiner, *Heavy Ion Physics* **1** 309 (1995).
56. J. Brachmann et al., to be published
57. H. Sorge, A. von Keitz, R. Mattiello, H. Stöcker, W. Greiner, *Phys. Lett.* **B243** 7 (1990).
58. M. Bleicher, N. Amelin, S.A. Bass, M. Brandstetter, A. Dumitru, C. Ernst, L. Gerland, J. Konopka, C. Spieles, H. Weber, L.A. Winckelmann, H. Stöcker, W. Greiner, in: *Proceedings of the International Conference on Nuclear Physics at the Turn of Millenium: Structure of Vacuum and Elementary Matter*, Wilderness/George, South Africa, 10-16, Mar 1996, p 452-457.